

Experimental Investigation of the Interaction of Water and Methanol with Anatase–TiO₂(101)

G. S. Herman,^{*,†,‡} Z. Dohnálek,^{*,†} N. Ruzycki,[§] and U. Diebold[§]

Environmental Molecular Sciences Laboratory, Pacific Northwest National Laboratory, P.O. Box 999, MSIN K8-93, Richland, Washington 99352, and Department of Physics, Tulane University, New Orleans, Louisiana 70118

Received: November 25, 2002; In Final Form: January 15, 2003

The interaction of water and methanol with well-defined (1×1) terminated surfaces of anatase-TiO₂(101) were investigated with temperature-programmed desorption (TPD) and X-ray photoelectron spectroscopy (XPS). For water, three desorption states were observed in the TPD spectra at 160, 190, and 250 K. The three desorption peaks were assigned to multilayer water, water adsorbed to 2-fold-coordinated O, and water adsorbed to 5-fold-coordinated Ti, respectively. The TPD spectra for methanol were more complicated. For methanol, five desorption peaks were observed in the TPD spectra at 135, 170, 260, 410, and 610 K. The five desorption peaks were assigned to multilayer methanol, methanol adsorbed to 2-fold-coordinated O, methanol adsorbed to 5-fold-coordinated Ti, methoxy adsorbed to 5-fold-coordinated Ti, and methoxy adsorbed to Ti at step edges, respectively. The XPS results indicated that the adsorbed water and methanol were predominantly bound to the surface in a molecular state, with no evidence for dissociation. Furthermore, the O 1s core-level binding energies for water and methanol were found to shift to an ~ 0.75 eV lower binding energy for coverages before multilayer desorption is observed in the TPD spectra. The O 1s core-level binding-energy shift appears to be linear in this region and corresponds to water and methanol bonding to Ti cation and O anion sites on the surface. The C 1s core-level binding energy for methanol was found to remain approximately constant in the same coverage regime.

I. Introduction

There has been much interest in the interaction of water and methanol with TiO₂ surfaces because of its unique photocatalytic properties.^{1,2} For example, the photocatalytic production of hydrogen from water was first observed on a rutile-TiO₂ single crystal in 1972.³ The photoinduced splitting of water to hydrogen and oxygen using visible light is considered to be an important environmentally benign strategy that is critical for the future “hydrogen” economy. A second TiO₂ application that has attracted considerable attention is the photocatalytic destruction of organic compounds in polluted water and air.² For fundamental investigations of such processes, methanol is considered to be a prototypical organic compound.⁴ For both types of reactions, TiO₂ is considered to be a very important material because of the relatively high photoactivities and stabilities in a variety of environments.

The three common polymorphs of TiO₂ include rutile, anatase, and brookite. Both rutile and anatase have been extensively investigated with respect to their interaction with water and methanol, and much of this work has been performed on polycrystalline materials.^{4–10} It has been shown that anatase is the more photoactive polymorph for the photocatalytic production of hydrogen from water and is the only polymorph that can produce hydrogen without applying an external bias.¹¹ The photocatalytic activity for the decomposition of organic molecules on TiO₂ is more complex and appears to depend strongly on both the molecule and the polymorph.¹²

Nearly all of the work published to date on TiO₂ single crystals has focused on rutile, in large part because of their commercial availability. Of the anatase single-crystalline surfaces investigated, the anatase (001) surface has received the most attention because of the ease of preparation and the fact that it reconstructs to a two-domain (1×4) reconstruction.^{13–21} Currently, no experimental evidence exists that indicates that (1×4) reconstruction is observed on (001) surfaces of polycrystalline/nanocrystalline powders; furthermore, the structural complexity of the reconstruction led us to investigate the anatase (101) surface. Previous studies have shown that the (101) surface is the predominant face that is exposed on anatase minerals and polycrystalline powders.²² Furthermore, theory confirms that the (101) surface of anatase is thermodynamically the low-energy surface.²³

As mentioned above, very little is known about the interaction of water or methanol with well-defined single-crystal anatase surfaces. An early study on anatase (101) indicated that the complete photoelectrolysis of water to molecular hydrogen and oxygen can occur when the anatase electrode is exposed to UV radiation with an energy greater than the band gap (3.2 eV).¹¹ An extension of this work has also compared the photoactivity of the (001) and (101) surfaces of anatase.²⁴ It was found that the two surfaces have different flat-band potentials where the (001) surface is found to be ~ 0.06 V more negative than the (101) surface, possibly because of the different adsorption state of water on these two surfaces.²⁴ Theoretical investigations suggested that water dissociates on the (001) surface of anatase and adsorbs molecularly on the (101) surface.²⁵ The only other experimental study on the interaction of water with a single-crystalline anatase surface indicated that rapid hydrophilic-to-hydrophobic transitions were possible on the (001) surface by

* Corresponding authors. E-mail: gs_herman@yahoo.com and zdenek.dohnalek@pnl.gov.

[†] Pacific Northwest National Laboratory.

[‡] Current address: Hewlett-Packard Company, Corvallis, Oregon 97330.

[§] Tulane University.

a mechanochemical treatment.²⁶ Hydrophobic-to-hydrophilic transitions on TiO₂ have been attributed to the dissociation of molecular water and the formation of hydroxyl groups at Ti³⁺ sites.²⁷ No experimental studies to date have studied the interaction of methanol with single-crystalline anatase.

In this study, we investigate the interaction of water and methanol with the anatase-TiO₂(101) surface using low-energy electron diffraction (LEED), temperature-programmed desorption (TPD), and X-ray photoelectron spectroscopy (XPS). We find that water adsorbs molecularly on the fully oxidized anatase (101) surface. For methanol, we find predominately molecular adsorption; however, dissociative adsorption occurs at defect sites. These results are compared to prior studies on polycrystalline anatase and single-crystalline rutile.

II. Experimental Section

The experiments were conducted in an ultrahigh vacuum (UHV) chamber with a base pressure of $\sim 2 \times 10^{-10}$ Torr. The samples were natural anatase single crystals that were irregularly shaped but were approximately 8×10 mm² in size. They were oriented to the (101) surface plane and polished. The bulk impurities included Zr, Al, K, and Mo with a total bulk concentration of less than 1% as estimated by XPS. To reduce the influence of the impurities on the surface chemistry, a homoepitaxial anatase-TiO₂(101) film was grown on top of the mineral sample. The growth of the homoepitaxial films has been reported elsewhere, and good low-energy and reflection high-energy electron diffraction patterns were observed.¹⁹ Furthermore, scanning tunneling microscopy (STM) indicated that flat domains can be obtained on these samples, and atomic resolution was observed.²⁸

We exposed the anatase surface to water or methanol using quasieffusive molecular beams²⁹ of either D₂O, H₂O, or CH₃-OH. The H₂O flux in the beam was determined from the known saturation coverage of H₂O on MgO(001)³⁰ and Pt(111)³¹ and the previously measured fluence required to achieve these coverages.³² The average H₂O flux determined from these two measurements is 1.7×10^{14} molecules/cm²/s. The CH₃OH flux was determined using the mass-dependent flux under the effusive beam conditions. The H₂O flux was multiplied by the square root of the H₂O to CH₃OH mass ratio and yields the CH₃OH flux to be 9.8×10^{13} molecules/cm²/s. The error bars on these exposures were estimated to be ca. $\pm 10\%$ on the basis of measurements from several different samples over a period of time. The sample was dosed at temperatures below ~ 130 K for all of the experimental results shown. A small-diameter beam (~ 3 mm) was used to ensure that only the front face of the sample was exposed to H₂O. Centering of the molecular beam on the sample was confirmed by a visual inspection of a macroscopically thick ice film.

The sample temperature was measured using a W-5% Re/W-26% Re thermocouple cemented (AREMCO) on the edge of the sample. A linear ramp rate of 1 K/s was used for the TPD experiments. The use of a mineral anatase crystal led to difficulties in obtaining good thermal contact between the sample and the mounting plate. Although the ramp of the sample was linear, the cooling took a considerable amount of time (~ 20 min), which led to the adsorption of some water from the background. We estimated that this background water exposure was less than 0.05 ML referenced to the 5-fold-coordinated Ti cation sites at the surface (5.2×10^{14} /cm²). The XPS measurements were performed using Mg K α radiation from a non-monochromated source. The hemispherical analyzer was a Physical Electronics Omni Focus III with variable apertures and a small-area lens. The XPS measurements were performed using

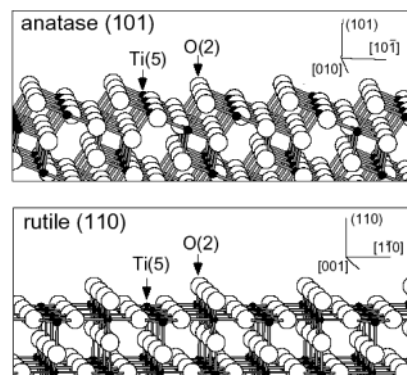


Figure 1. Schematic representation of the anatase (101) and the rutile (110) surfaces, top and bottom, respectively. The large open circles represent oxygen anions, and the small filled circles represent titanium cations.

a 1.1-mm diameter spot, a take-off angle of 60° with respect to the surface normal, and a pass energy of 11.75 eV. The binding-energy scale was referenced to the binding energy of the Au 4f_{7/2} ($E_b = 84.0$ eV) peak obtained from a foil in contact with the substrate.

III. Results

The two low-energy surfaces for TiO₂, the (101) surface of anatase, and the (110) surface of rutile are shown in Figure 1a and b, respectively. The small dark circles represent Ti cations, and the large light circles represent O anions. These two surfaces are similar in several ways. For instance, both surfaces have 5-fold-coordinated Ti cations and 2-fold-coordinated O anions with a surface concentration of $\sim 5.2 \times 10^{14}$ sites/cm² for each species on both crystallographic planes (5.16×10^{14} sites/cm² for anatase and 5.20×10^{14} sites/cm² for rutile). Both 6-fold-coordinated Ti cations and 3-fold-coordinated O anions make up the remainder of the sites for both surfaces. A significant difference between the two surface terminations are that the anatase surface has a sawtooth profile in which the 2-fold-coordinated O anions are bound to the 5-fold-coordinated Ti cations, whereas the rutile surface is flat with 2-fold-coordinated bridging oxygens bound to 6-fold-coordinated Ti cations and are projected out of the surface plane. Removal of one 2-fold-coordinated bridging oxygen results in two 4-fold-coordinated Ti³⁺ cations and two 5-fold-coordinated Ti³⁺ cations for the anatase and rutile surfaces, respectively. These highly under-coordinated Ti cations for anatase are likely to be less stable than the Ti cations for rutile and may explain why the number of oxygen vacancies observed by STM at the surface of anatase (101) is much lower than that observed for rutile (110).²⁸

In Figure 2, we show the TPD results for D₂O adsorbed on the anatase (101) surface for coverages between 0 and 15.3×10^{14} molecules/cm² with 1.7×10^{14} molecules/cm² dosed per step. Molecular water was the only species that was observed to desorb from the surface. It was found that integrating the D₂O desorption peaks and plotting this intensity versus the dose gave a straight line that passes through the origin, indicating unity sticking coefficient of D₂O on anatase (101). This is in agreement with direct sticking coefficient measurements (data not shown) by a King and Wells technique with the sample at 100 K.³³ For low coverages, there is a broad peak between 210 and 290 K, which saturates for coverages of $\sim 5 \times 10^{14}$ molecules/cm² with a desorption temperature of ~ 250 K. This coverage is approximately equal to the number of 5-fold-coordinated Ti cation or 2-fold-coordinated O anion sites on the anatase (101) surface. Increasing the water coverage results

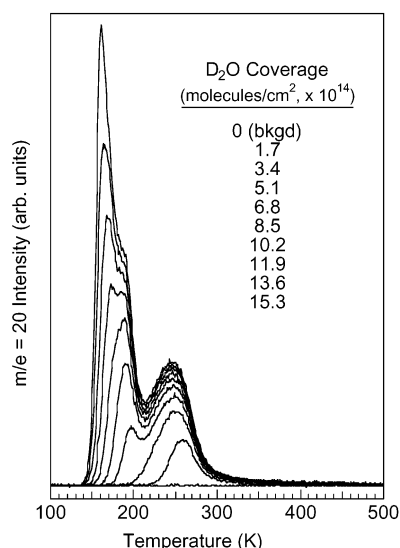


Figure 2. D_2O TPD spectra ($m/e = 20$ amu) are shown for the anatase (101) surface for coverages between 0 and 15.3×10^{14} molecules/cm² with 1.7×10^{14} molecules/cm² dosed per step.

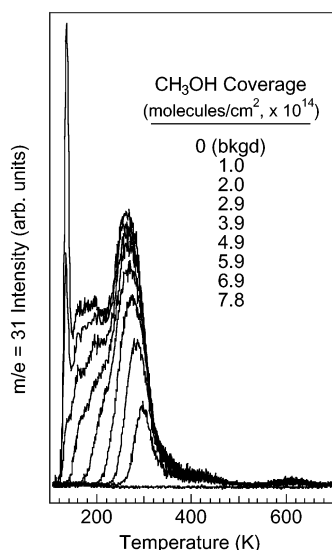


Figure 3. CH_3OH TPD spectra ($m/e = 31$ amu) are shown for the anatase (101) surface for coverages between 0 and 7.8×10^{14} molecules/cm² with 9.8×10^{13} molecules/cm² per step.

in the saturation of a second desorption state at ~ 190 K for a coverage of $\sim 1 \times 10^{15}$ molecules/cm². Finally, for higher water coverages, a low-temperature desorption state appears at ~ 160 K and is found to increase in intensity with increasing coverages. In the following discussion, we define the completion of the first monolayer as the coverage required to saturate the 250 K desorption state, the completion of the second monolayer as the coverage required to saturate the 190 K desorption state, and higher coverages as a multilayer state.

In Figure 3, we show the TPD ($m/e = 31$) results for methanol adsorbed on the anatase (101) surface for coverages between 0 and 7.8×10^{14} molecules/cm² with 9.8×10^{13} molecules/cm² per step. Similar to the case of water adsorption, integration of the methanol TPD area resulted in a straight line passing through the origin. This indicates a unity sticking coefficient of methanol on anatase (101) in agreement with a direct sticking coefficient measurement (data not shown) using a King and Wells technique with the sample at 100 K.³³ The absence of a C 1s peak in the XPS spectrum after the TPD experiment confirmed that the entire dose of methanol desorbed from the surface. For low

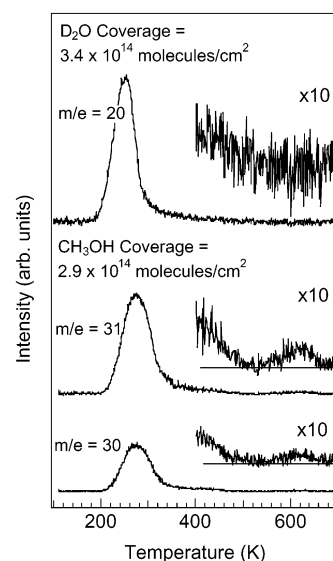


Figure 4. TPD spectra from a vacuum-annealed anatase (101) sample for a D_2O coverage of 3.4×10^{14} molecules/cm² ($m/e = 20$) (upper) and for a CH_3OH coverage of 2.9×10^{14} molecules/cm² ($m/e = 30$ and 31) (lower).

coverages, we observe the saturation of small TPD peaks at 610 and 410 K. Increasing the methanol coverage up to $\sim 4 \times 10^{14}$ molecules/cm² results in the saturation of a broad peak at 260 K. Higher coverages, up to $\sim 6 \times 10^{14}$ molecules/cm², resulted in the formation of a broad TPD peak centered between 155 and 190 K. Further dosing leads to the formation of methanol multilayers with a TPD peak at ~ 135 K. In the following discussion, we define the completion of the first monolayer as the coverage required to saturate the 260 K desorption state, the completion of the second monolayer as the coverage required to saturate the 155–190 K desorption state, and higher coverages as a multilayer state.

To compare the TPD spectra directly for water and methanol from the anatase surface, we show the high-temperature region for both molecules in Figure 4. In both cases, the sample was vacuum annealed up to ~ 800 K and exposed to $\sim 3 \times 10^{14}$ molecules/cm². It is clear that no high-temperature desorption states exist for water, whereas a state at 610 K is clearly evident for methanol for both m/e equal to 30 and 31. These m/e values of 30 and 31 were used to determine whether methanol was oxidized to formaldehyde on the anatase surface. For example, m/e 30 has contributions from both formaldehyde and methanol, whereas m/e 31 has a contribution from only methanol. Both m/e 30 and 31 are identical in shape and relative intensities, indicating that no formaldehyde is formed on this surface. To determine whether this high-temperature desorption state was from the sample, we have performed control experiments using an identical methanol exposure with the sample out of the path of the molecular beam. No evidence of the 610 K desorption feature was found in the TPD, confirming that this state originates from the anatase (101) surface.

To gain further insight into the interaction of the adsorbed water with the anatase surface, we have performed XPS for several coverages at 130 K. These data are shown in Figure 5 with the water coverage indicated. The substrate O 1s binding energy was 531.0 eV and was found to change by less than ± 0.05 eV with increasing water coverage. A second peak related to adsorbed H_2O was observed at higher binding energy (~ 534.5 eV), with the intensity increasing nearly linearly up to 2 ML. Interestingly, the O 1s peak due to water was found to shift to lower binding energies by ~ 1 eV for increasing coverage up

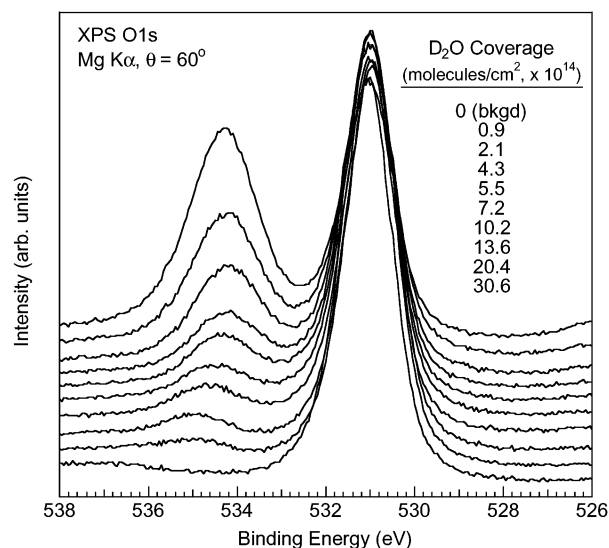


Figure 5. O 1s spectra are shown for the anatase (101) surface for water coverages between 0 and 3.06×10^{15} molecules/cm².

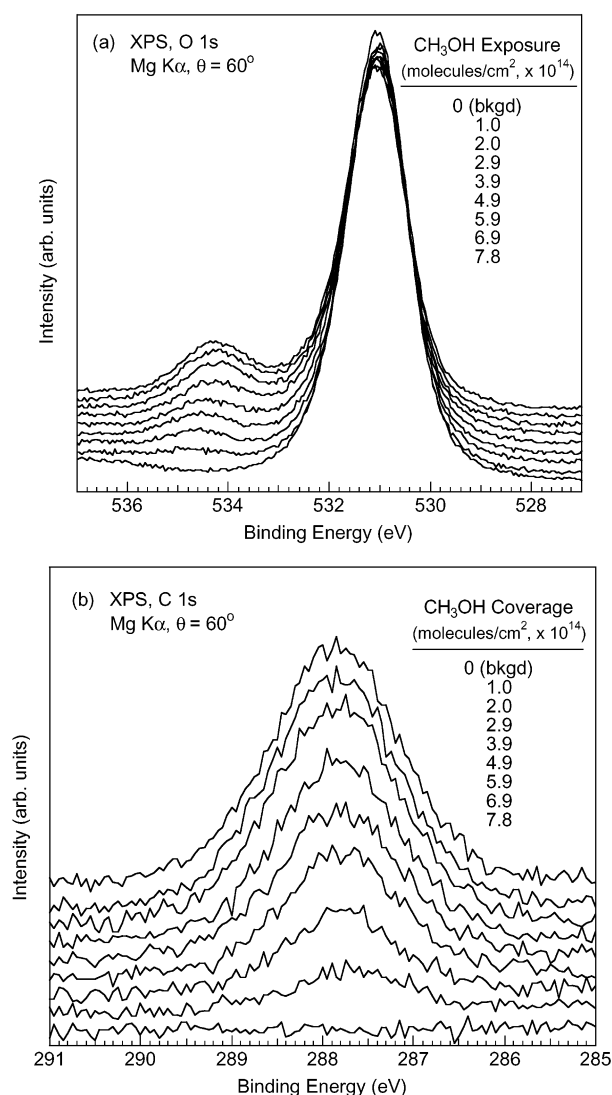


Figure 6. (a) O 1s and (b) C 1s spectra are shown for the anatase (101) surface for methanol coverages between 0 and 7.8×10^{14} molecules/cm².

to 2 ML. No changes in the O 1s fwhm were observed in these measurements.

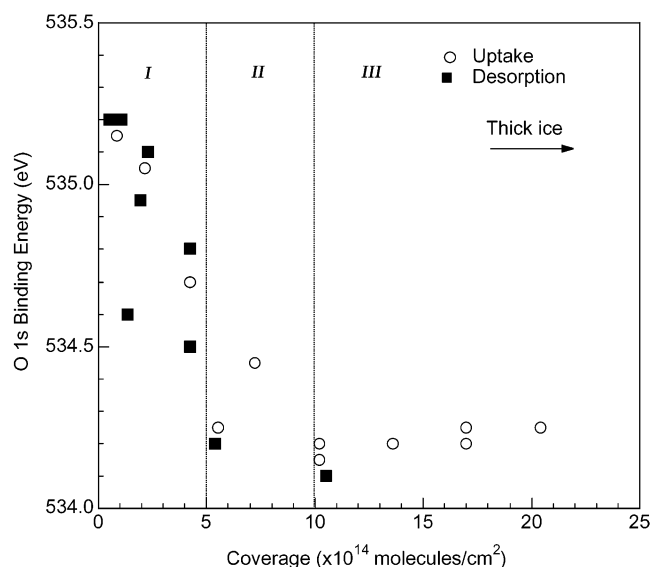


Figure 7. Binding energy of the O 1s peak of adsorbed water relative to coverage. Open circles (“uptake”) represent values for as-adsorbed water layers. Filled squares (“desorption”) represent data for water coverages obtained by the adsorption of a thicker layer at 130 K and subsequent heating to higher temperatures. Indicated with thin lines are the saturation coverages for the TPD features at 260 K and 155–190 K. The value for a thick layer of water (“ice”) is also indicated.

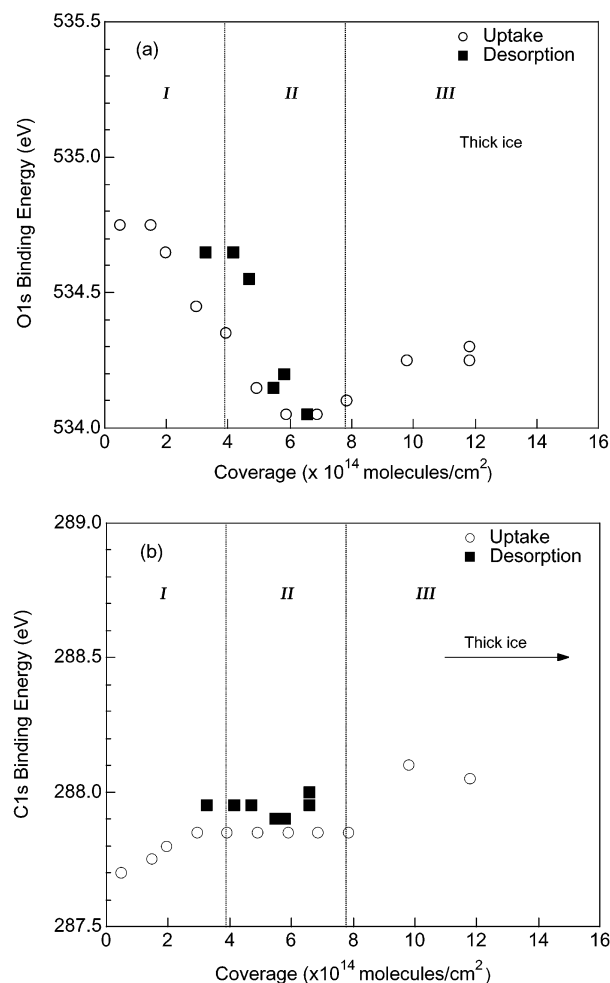
For methanol, we have obtained XPS results for O 1s and C 1s emission for a variety of coverages on anatase (101) at 130 K as shown in Figure 6a and b, respectively. With increasing coverage, the methanol O 1s and C 1s XPS peaks were found to increase linearly in intensity, and the substrate O 1s and Ti 2p XPS peaks were found to decrease linearly in intensity. The binding energy of the O 1s peak due to methanol was found to shift to lower binding energies by ~ 0.75 eV for increasing coverages up to 2 ML, similar to what was observed for water. In contrast, the binding energy of the C 1s peak increases slightly for very low coverages and then remains approximately constant. Samples that initially had $\sim 7.8 \times 10^{14}$ molecules/cm² at 130 K and were subsequently annealed to various temperatures showed similar trends.

The binding energy of the water O 1s peak as a function of water coverage at 130 K is shown as open circles in Figure 7. Coverage regions I, II, and III are indicated in Figure 7 and correspond to the coverages required to fill the 250, 190, and 160 K desorption peaks in Figure 2, respectively. For the purpose of extracting the water O 1s peak binding energy, we have subtracted the overlapping substrate O 1s satellite peak at 535 eV. Analogous data obtained for anatase with multilayer initial coverages and subsequent ramps to various temperatures between 155 and 450 K are shown as filled squares in Figure 7. The amount of water remaining on the surface was calculated from the area in the representative TPD spectrum above the corresponding annealing temperature. Both sets of data are found to fall on one common curve. The O 1s peak shifts to lower binding energies by ~ 1 eV for increasing coverages up to 2 ML. The maximum of the downward shift is reached at the onset of multilayer adsorption at a water coverage of $\sim 1 \times 10^{15}$ molecules/cm².

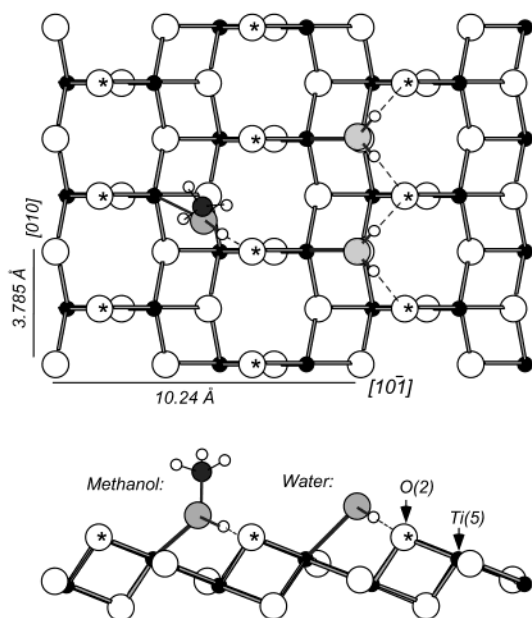
Variations in the O 1s and C 1s binding energies with respect to methanol coverages at 130 K are shown as open circles in Figure 8a and b, respectively. Coverage regions I, II, and III are indicated in Figure 8a and b and correspond to the coverages required to fill the 260, 155–190, and 135 K desorption peaks in Figure 3, respectively. Again, for the purpose of extracting

TABLE 1: Desorption Temperatures for Water and Methanol from Anatase (101) and Rutile (110) Surfaces with Their Respective Binding Sites

water		methanol		comment
anatase (101), ^a K	rutile (110), ^b K	anatase (101), ^a K	rutile (110), ^c K	
160	155	135	145	molecular multilayer desorption
190	160–180	170	165	molecular hydrogen bonding to O(2)
250	270	260	295	molecular bonding to Ti(5)
		410	350	dissociated bonding to Ti(5)
	490–520		480	dissociated bonding to oxygen vacancy sites
		610		dissociated bonding to step edges

^a Present study. ^b References 34–36. ^c Reference 44.**Figure 8.** Binding energy of the (a) O 1s and (b) C 1s peaks of adsorbed methanol relative to coverage. Open circles (“uptake”) represent values for as-adsorbed methanol layers. Filled squares (“desorption”) represent data for methanol coverages obtained by the adsorption of a thicker layer at 130 K and subsequent heating to higher temperatures. Indicated with thin lines are the saturation coverages for the TPD features at 260 K and 155–190 K. The value for a thick layer of methanol (“ice”) is also indicated.

the methanol O 1s peak binding energy, we have subtracted the overlapping substrate O 1s satellite peak at 535 eV. The O 1s and C 1s peak binding energies for anatase with multilayer initial coverages and subsequent ramps to various temperatures between 125 and 560 K are shown as filled squares in Figure 8a and b, respectively. The amount of methanol remaining on the surface was calculated by integrating the area in the representative TPD spectrum above the annealing temperature. Both sets of O 1s data are found to fall on one common curve with O 1s peak shifts to lower binding energies by ~ 0.75 eV for increasing coverages up to 2 ML. The maximum of the

**Figure 9.** Top view (upper) and side view (lower) of possible adsorption geometries of methanol (left) and water (right) on anatase (101). Large white balls: substrate oxygen (bridging oxygen atoms are marked with stars); small black balls: substrate titanium; large gray balls: oxygen of the adsorbates; small white balls: hydrogen of the adsorbate; large black balls: carbon of the adsorbate.

downward shift is reached at the onset of multilayer adsorption at coverages around $\sim 6 \times 10^{14}$ molecules/cm². In contrast, the methanol C 1s binding energy was found to remain fairly constant in the same coverage regime.

IV. Discussion

Water TPD. The water TPD spectra for the anatase (101) surface are very similar to those reported in the literature for the rutile (110) surface.^{34–36} The major differences are slight shifts in desorption temperatures and the missing peak at ~ 500 K that has been assigned to water adsorption and dissociation at bridging oxygen vacancy sites for the rutile (110) surface.^{34–38} The resulting water desorption temperatures for the anatase (101) surface and literature values for rutile (110) are indicated in Table 1 with assignments to the specific binding states. The high-temperature desorption state for anatase (101) is ~ 250 K, which we assign to water bonding to the 5-fold-coordinated Ti cation site as shown in Figure 1. Theoretical studies have indicated that water is molecularly adsorbed on the anatase (101) surface and that the nucleophilic end (oxygen) is bound to the 5-fold-coordinated Ti cation site and the hydrogens form hydrogen bonds with the bridging oxygens of neighboring acid–base pairs.²⁵ The predicted water binding site is illustrated in the right portion of Figure 9. Upon increasing the number of water molecules from 0.25 to 1 ML in the calculations, very

little change in adsorption energy was observed, with a decrease from 0.74 to 0.72 eV. Performing a Redhead analysis³⁹ with a preexponential of 10^{13} on the TPD spectra in Figure 3, we find that the desorption energy of H₂O on 5-fold-coordinated Ti sites shifts from 0.69 to 0.65 eV for increasing coverage. The desorption energy provides a good estimate of the molecular binding energy for nonactivated adsorption, which we assumed in this analysis. Thus, good agreement between the experimental and theoretical coverage-dependent binding-energy shift was obtained.

Our assignment for anatase appears to be in good agreement with the assignment for rutile (110). For example, rutile (110) has a water desorption peak at ~ 270 K that is assigned to the desorption of water from the 5-fold-coordinated Ti cation. On rutile (110), the experimental desorption energy of H₂O on 5-fold-coordinated Ti sites shifts from 0.74 to 0.64 eV for increasing coverage,³⁴ which is slightly higher than what we observed on anatase (101).

At higher coverages, we also observe a second desorption state at 190 K, which we assign to molecular water hydrogen bonded to 2-fold-coordinated O anion sites on the anatase (101) surface. The Redhead analysis³⁹ using a preexponential of 10^{13} yields a H₂O desorption energy of ~ 0.5 eV. Although there are no theoretical predictions of the binding energy for this state, water desorption from oxygen-terminated surfaces result in similar desorption temperatures.^{40,41} Furthermore, a similar assignment was made for the 160–180 K water desorption state from rutile (110).

Finally, the desorption state at 160 K is known to be due to water desorption from multilayers.⁴² Although the data shown in Figure 2 are very similar to prior data from rutile (110), there are several differences. First, the 250 K state is ~ 25 K lower in temperature than the desorption state from rutile (110), suggesting weaker water-to-Ti cation bonding for anatase or less stabilization of the water molecule by hydrogen bonding to bridging oxygen ions. Second, the 190 K state is ~ 10 – 30 K higher in temperature than the desorption state from rutile (110), suggesting stronger water-to-O anion bonding for anatase. Third, no higher-temperature desorption states were observed in these experiments even though the surface was flashed to 850–900 K in UHV between each run. (See Figure 4.) Likewise, for rutile (110), it was found that the formation of oxygen vacancies by an ~ 850 K annealing resulted in a high-temperature desorption state centered at ~ 500 K. A prior theoretical study has suggested that anatase is more difficult to reduce than rutile.⁴³ This finding has recently been confirmed by STM²⁸ and is in agreement with our water TPD presented here.

A prior UHV-TPD study performed on rutile and anatase powders has also shown that the water desorbs at very similar temperatures for these two polymorphs.⁶ Although several different crystal faces are present on the anatase and rutile powders, the (101) and (110) surfaces, which are thermodynamically the lowest-energy surfaces for anatase and rutile, respectively, are expected to be dominant.²² The water TPD from anatase powders resulted in desorption peaks at 180, 222, and 312 K whereas those from rutile resulted in desorption peaks at 180, 211, 311, and 568 K. It was confirmed by FTIR spectroscopy that the high-temperature state on rutile is related to dissociated water. The results from single-crystal anatase (101) and rutile (110) reproduce these powder results very well since water is not found to dissociate on anatase (101), apparently because of the absence of oxygen-vacancy defect sites.

Methanol TPD. Overall, the methanol TPD results from anatase (101) are qualitatively very similar to those from rutile (110).⁴⁴ Furthermore, our methanol TPD data from an 850 K annealed anatase (101) surface more closely match those from an oxidized rutile (110) surface^{44,45} rather than those from an 850 K annealed rutile (110) surface.^{44,46,47} This is not unexpected since our water TPD from anatase (101) indicates the absence of oxygen-vacancy adsorption sites for water. The resulting methanol desorption temperatures for the anatase (101) surface and literature values for vacuum-annealed rutile (110) are indicated in Table 1 with assignment to the specific binding states. The desorption peak observed for anatase at 260 K is assigned to molecular methanol bound to 5-fold-coordinated Ti cation sites and is illustrated in Figure 9. Typical bond lengths and angles for methanol adsorption have been taken from ref 48. The CH₃ group, drawn upright in this schematic, is expected to rotate toward the substrate. The desorption peak between 155 and 190 K is assigned to molecular methanol bound to 2-fold-coordinated O anion sites. These two desorption states are also observed for rutile (110) and occur at 295 and 165 K, respectively. For anatase and rutile, the saturation coverages for the 260 and 295 K desorption states were estimated to be 4×10^{14} and 3×10^{14} molecules/cm², respectively. Furthermore, the dissociation of methanol appears to occur on both the anatase and rutile surfaces at 5-fold-coordinated Ti cation sites where these desorption temperatures are 410 and 350 K, respectively. The major difference between vacuum-annealed anatase (101) and vacuum-annealed rutile (110) is that anatase has a high-temperature desorption state at 610 K whereas rutile has a high-temperature desorption state at 480 K. For anatase, we assign this state to methoxy species adsorbed to step edges, and for rutile, this state was assigned to methoxy species adsorbed to bridging vacancy sites. For an oxidized rutile (110) surface, a desorption state at ~ 625 K is observed.⁴⁴ On the basis of the differences in *m/e* 29 and 31 TPD spectra, it was estimated that both formaldehyde and methanol desorb at 625 K as a result of a disproportionation reaction between two methoxy groups. It has been previously shown that the oxidized rutile (110) surface can form rough surfaces with hexagonal rosettes and strands,⁴⁹ and it was suggested that these structures are where the high-temperature methoxy groups bond. For anatase, we monitored *m/e* 30 and 31, shown in Figure 4, and found that the overall shape and relative intensities for the two TPD spectra were identical over the entire temperature range. This suggests that *m/e* 30 and 31 are both due to the cracking of methanol and that no formaldehyde is formed on this surface even for the high-temperature state. This result suggests that the condensation of hydroxyl groups (produced in the course of the dissociative adsorption of methanol) does not occur on anatase, possibly because of the difficulty in removing a lattice oxygen from the anatase (101) surface. Our TPD measurements estimate that the intensity of the 610 K methanol feature is ~ 0.02 ML, which coincides with the number of possible adsorption states at step edges based on quantitative STM studies.²⁸

The TPD of methanol from anatase and rutile powder samples has been previously studied.^{8,9} The TPD spectra of anatase and rutile powders were very similar to one another, with the major differences related to the selectivities for the reaction products. Methanol desorption for both anatase and rutile was centered at ~ 400 K, and no high-temperature desorption state was observed. However, dimethyl ether, formaldehyde, and methane were observed to desorb from both anatase and rutile for temperatures above 600 K. It was suggested that dimethyl ether is formed by a bimolecular dehydration of two methoxy species

on both anatase and rutile. On the basis of studies on rutile (001),⁵⁰ doubly coordinated unsaturated surface cations are required to produce dimethyl ether. Dimethyl ether desorption from anatase (101) was not explored in detail in our experiments. However, as mentioned earlier, the 610 K methanol TPD peak corresponds to a coverage of ~ 0.02 ML. Furthermore, the C 1s and O 1s XPS measurements from a saturated surface that has been heated to 560 K indicate that no carbon-containing species are present above the noise level in the experiments, which is consistent with a coverage < 0.05 ML. When combined, these results suggest that dimethyl ether is not a major desorption product from the anatase (101) surface.

Water XPS. As shown in Figure 7, there is a considerable shift in the water O 1s binding energy with coverage. For submonolayer coverages up to the completion of the first and second monolayers of water (i.e., water bound to 5-fold Ti and 2-fold O sites), a binding-energy shift from 535.2 to 534.2 eV is observed. In a prior XPS study of water on rutile (110), a water O 1s binding energy of 532.9 eV was determined, and this peak position did not shift significantly when a sample dosed with a 1.5 ML of water was flashed to 185 and 300 K.³⁴ The water state on rutile (110) was assigned to molecular water.³⁴ Dissociated water is known to have a lower binding energy than molecular water, which leads us to assign the species adsorbed on anatase (101) as molecular water.^{34,51,52} The binding-energy shift observed in Figure 7 is nearly linear with coverage for low coverages (i.e., bound only to 5-fold Ti sites) up to the completion of the second layer (i.e., bound to both 5-fold Ti and 2-fold O sites). To confirm that the water was not clustering while absorbing at low temperatures, we have performed annealing experiments in which saturated water layers are flashed up to several temperatures, and XPS data are obtained. Calibrating the remaining water left on the surface with our TPD experiments indicates that adsorption and desorption experiments give identical binding energies for the water O 1s peak with respect to water coverage. These results suggest that there is no change in the binding state of water at the surface as deposited at 130 K and after annealing to the specified temperatures.

Core-level shifts of this magnitude can typically be assigned to changes in the chemical state of the adsorbate; however, on the basis of the observed binding energies for the adsorbed water, it is very unlikely that dissociation with the formation of hydroxyl groups takes place on this surface with a significant coverage. Initial-state chemical shifts related to a change in the nature of the water bonding at the surface with increasing coverage (e.g., $\text{H}_2\text{O}-\text{Ti}_{(\text{s})} \rightarrow \text{H}_2\text{O}-\text{O}_{(\text{s})} \rightarrow \text{H}_2\text{O}-\text{H}_2\text{O}$) can also be considered, although it is difficult to rationalize linear behavior in the binding energy versus coverage plot in Figure 7 when water is adsorbed at both Ti 5-fold and O 2-fold sites and both sites are being filled sequentially. That is, we would expect a change in the slope, at $\sim 5 \times 10^{14}$ molecules/cm², when the water transitions from lone-pair electrons on the water oxygen atom interacting with the Ti cation empty states and the hydrogen–oxygen bond in the water molecule lengthens because of hydrogen bonding to a substrate oxygen anion. These two chemical binding states appear to be very different from one another, and we would expect them to have very different binding energies for the O 1s core level. In fact, considering only initial-state effects, the O 1s binding energy for water bonded to Ti cations (water as an electron donor) would likely shift in the opposite direction compared to that of water hydrogen bonded to bridging oxygens (water as an electron acceptor). A recent theoretical study indicated that increasing

the hydrogen–oxygen bond length, related to hydrogen bonding with another water molecule, results in a considerable decrease in the oxygen core-level binding energy.⁵³ Changes in the final-state screening due to interactions with other molecules or the surface can also be considered in regard to the shift in binding energy. It is difficult to determine whether the observed shifts for the first two monolayers are related to final-state screening effects. Again, we would not necessarily expect a single slope dependence when going from 0 to 1×10^{15} molecules/cm². For monolayer-to-multilayer water coverages, the binding-energy shift is expected to increase for molecules further from the surface because of decreased screening from the surface and is clearly seen in our data for multilayer coverages. Certainly more experiments are necessary to identify the exact nature of the water interactions at low coverages.

Methanol XPS. To determine whether a dissociative adsorption of methanol occurs on the anatase (101) surface, we have compared our C 1s binding energies to those obtained from rutile (001).⁵⁰ However, to better compare the relative numbers from these two studies, we will compare the difference between the observed Ti 2p_{3/2} and C 1s core levels to reduce errors due to possible band-bending or charging effects. The prior study on rutile gave binding-energy differences of 172.1 and 172.7 eV for methanol and methoxy, respectively. For our study, the difference in the Ti 2p_{3/2} binding energy and the C 1s binding energy is 171.9 eV, which is in excellent agreement with that of adsorbed molecular methanol. We observed very little change in this value with respect to coverage or annealing temperature. Interestingly, our O 1s core-level peaks shift much like those observed for water. Again, we are not able to identify the precise cause of these shifts; however, it is interesting that XPS measurements taken from methanol adsorbed on a Ag(111) surface gave only very small shifts with increasing binding energy for methanol C 1s and O 1s core-level peaks.⁵⁴

In general, the XPS results for water and methanol on anatase (101) suggest that the molecule–surface interactions may strongly influence the core-level binding energies for the O 1s core level. Furthermore, the C 1s core level was found to be much less sensitive to methanol surface coverage. Certainly this is expected since the binding interactions are through either the oxygen atom on titanium sites or through the hydrogen atom on oxygen sites. Recent work has suggested that hydrogen bonding can change the relative binding energy of complex molecules on rutile (110) surfaces; however, these authors primarily investigated the N 1s core level in these molecules.⁵⁵ Typically, very little analysis is done on the O 1s core levels for oxygen-containing molecules adsorbed on oxides at submonolayer coverages, which may be due to the fact that the molecular signal is expected to be quite low compared to the substrate signal.^{51,56} This makes it difficult to determine if what we observe on anatase (101) is unique to this material. However, in a prior study of water on rutile (110), the authors did not observe these types of O 1s core-level shifts for submonolayer coverages.³⁴

Conclusions

The interaction of water and methanol with the anatase (101) surface was found to be different compared to what has been previously observed for rutile (110). The major differences are related to the difficulty in forming oxygen vacancy defects on anatase (101) as opposed to forming them on rutile (110). This difference can most notably be observed by the absence of a water or methanol desorption feature at ~ 500 K for the anatase (101) surface. We propose that it is more difficult to form

oxygen vacancies at the bridging oxygen rows of anatase (101) compared to rutile (110) because of differences in the coordination of the remaining reduced Ti cations. The water TPD patterns from oxidized rutile (110) look very much like those from anatase (101) with the only differences related to the temperatures for the specific desorption states. Overall, the methanol TPD spectra from oxidized rutile (110) look like those from anatase (101); however, we did not find evidence for the oxidation of methanol to formaldehyde in our experiments. Our XPS results indicated a unique shift in the O 1s core level, which warrants further study. Ultimately, the molecular binding, thermal chemistry, and electronic changes in the water and methanol molecules indicate that anatase (101) is different from rutile (110). This suggests that investigations on anatase are warranted if detailed molecular-level information related to specific reactions that are found to occur on anatase but not rutile (i.e., the photocatalytic production of hydrogen from water without an external bias) is desired.

Acknowledgment. We gratefully acknowledge Y. Gao of Agere Optoelectronics Center for growing the epitaxial films, J. Post of the Smithsonian Institute for providing the anatase mineral sample, and B. D. Kay and M. A. Henderson of Pacific Northwest National Laboratory (PNNL) for stimulating discussions. This research was supported by the PNNL Laboratory Directed Research and Development program. Z.D. gratefully acknowledges support from the U.S. DOE Office of Basic Energy Sciences, Chemical and Materials Science Division. PNNL is operated for the U.S. DOE by Battelle Memorial Institute under contract number DE-AC06-76RLO 1830. The research described in this paper was performed at the Environmental Molecular Sciences Laboratory, a national scientific user facility sponsored by the DOE Office of Biological and Environmental Research located at PNNL. U.D. and N.R. acknowledge support from a DOE grant under contract number DE-FGOL-00ER45834.

References and Notes

- Linsebigler, A. L.; Lu, G.; Yates, J. T. *Chem. Rev.* **1995**, 95, 735.
- Hoffmann, M. R.; Martin, S. T.; Choi, W.; Bahnemann, D. W. *Chem. Rev.* **1995**, 95, 69.
- Fujishima, A.; Honda, K. *Nature (London)* **1972**, 238, 38.
- Chuang, C.-C.; Chen, C.-C.; Lin, J.-L. *J. Phys. Chem. B* **1999**, 103, 2439.
- Jones, P.; Hockey, J. A. *J. Chem. Soc., Faraday Trans. 1* **1972**, 68, 907.
- Beck, D. D.; White, J. M.; Radcliffe, C. T. *J. Phys. Chem.* **1986**, 90, 3123.
- Ichikawa, S.; Doi, R. *Thin Solid Films* **1997**, 292, 130.
- Kim, K. S.; Barteau, M. A.; Farneth, W. E. *Langmuir* **1988**, 4, 533.
- Lusvardi, V. S.; Barteau, M. A.; Farneth, W. E. *J. Catal.* **1995**, 153, 41.
- Taylor, E. A.; Griffin, G. L. *J. Phys. Chem.* **1988**, 92, 477.
- Kavan, L.; Gratzel, M.; Gilbert, S. E.; Klemenz, C.; Scheel, H. J. *J. Am. Chem. Soc.* **1996**, 118, 6716.
- Mills, A.; Leहुnte, S. *J. Photochem. Photobiol. A* **1997**, 108, 1.
- Durinck, G.; Poelman, H.; Clauws, P.; Fiermans, L.; Vennik, J.; Dalmai, G. *Solid State Commun.* **1991**, 80, 579.
- Poelman, H.; Devriendt, K.; Fiermans, L.; Dewaele, O.; Heyndrickx, G.; Froment, G. F. *Surf. Sci.* **1997**, 377–379, 819.
- Chen, S.; Mason, M. G.; Gysling, H. J.; Paz-Pujalt, G. R.; Blanton, T. N.; Castro, T. N.; Chen, K. M.; Fictorie, C. P.; Gladfelter, W. L.; Franciosi, A.; Cohen, P. I.; Evans, J. F. *J. Vac. Sci. Technol. A* **1993**, 11, 2419.
- Herman, G. S.; Gao, Y.; Tran, T. T.; Osterwalder, J. *Surf. Sci.* **2000**, 447, 201.
- Herman, G. S.; Sievers, M. R.; Gao, Y. *Phys. Rev. Lett.* **2000**, 84, 3354.
- Hengerer, R.; Bolliger, B.; Erbudak, M.; Grätzel, M. *Surf. Sci.* **2000**, 460, 162.
- Herman, G. S.; Gao, Y. *Thin Solid Films* **2001**, 397, 157.
- Lazzeri, M.; Selloni, A. *Phys. Rev. Lett.* **2001**, 87, 266105/1.
- Liang, Y.; Gan, S.; Chambers, S. A.; Altman, E. I. *Phys. Rev. B* **2001**, 63, 235402/1.
- Oliver, P. M.; Watson, G. W.; Kelsey, E. T.; Parker, S. C. *J. Mater. Chem.* **1997**, 7, 563.
- Lazzeri, M.; Vittadini, A.; Selloni, A. *Phys. Rev. B* **2001**, 63, 155409 and references therein.
- Hengerer, R.; Kavan, L.; Krtil, P.; Gratzel, M. *J. Electrochem. Soc.* **2000**, 147, 1467.
- Vittadini, A.; Selloni, A.; Rotzinger, F. P.; Gratzel, M. *Phys. Rev. Lett.* **1998**, 81, 2954.
- Kamei, M.; Mitsuhashi, T. *Surf. Sci.* **2000**, 463, L609.
- Sakai, N.; Wang, R.; Fujishima, A.; Watanabe, T.; Hashimoto, K. *Langmuir* **1998**, 14, 5918.
- Hebenstreit, W.; Ruzycski, N.; Herman, G. S.; Gao, Y.; Diebold, U. *Phys. Rev. B* **2000**, 62, R16334.
- Dohnálek, Z.; Kimmel, G. A.; Ciolli, R. L.; Stevenson, K. P.; Smith, R. S.; Kay, B. D. *J. Chem. Phys.* **2000**, 112, 5932.
- Ferry, D.; Glebov, A.; Senz, V.; Suzanne, J.; Toennies, J. P.; Weiss, H. *Surf. Sci.* **1997**, 377–379, 634.
- Glebov, A.; Graham, A. P.; Menzel, A.; Toennies, J. P.; Senet, P. *J. Chem. Phys.* **2000**, 112, 11011.
- Dohnálek, Z. Unpublished work.
- King, D. A.; Wells, M. G. *Surf. Sci.* **1972**, 29, 454.
- Hugenschmidt, M. B.; Gamble, L.; Campbell, C. T. *Surf. Sci.* **1994**, 302, 329.
- Henderson, M. A. *Surf. Sci.* **1996**, 355, 151. Henderson, M. A. *Langmuir* **1996**, 12, 5093.
- Lu, G.; Linsebigler, A.; Yates, J. T. *J. Phys. Chem.* **1994**, 98, 11733.
- Brookes, I. M.; Murny, C. A.; Thornton, G. *Phys. Rev. Lett.* **2001**, 87, 266103.
- Schaub, R.; Thosttrup, P.; Lopez, N.; Laegsgaard, E.; Stensgaard, I.; Norskov, J. K.; Besenbacher, F. *Phys. Rev. Lett.* **2001**, 87, 266104.
- Redhead, P. A. *Vacuum* **1962**, 12, 203.
- Vurens, G. H.; Maurice, V.; Salmeron, M.; Somorjai, G. A. *Surf. Sci.* **1992**, 268, 170.
- Zhang, R.; Ludviksson, A.; Campbell, C. T. *Surf. Sci.* **1993**, 289, 1.
- Henderson, M. A. *Surf. Sci. Rep.* **2002**, 46, 1.
- Woning, J.; Van Saten, R. A. *Chem. Phys. Lett.* **1983**, 101, 541.
- Henderson, M. A.; Otero-Tapia, S.; Castro, M. E. *Faraday Discuss.* **1999**, 114, 313.
- Wang, Q.; Madix, R. J. *Surf. Sci.* **2001**, 474, L213.
- Wong, G. S.; Kragten, D. D.; Vohs, J. M. *Surf. Sci.* **2000**, 52, L293.
- Wong, G. S.; Kragten, D. D.; Vohs, J. M. *J. Phys. Chem. B* **2001**, 105, 1366.
- Bates, S. P.; Gillan, M. J.; Kresse, G. *J. Phys. Chem. B* **1998**, 102, 2017.
- Li, M.; Hebenstreit, W.; Diebold, U. *Surf. Sci.* **1998**, 414, L951.
- Kim, K. S.; Barteau, M. A. *Surf. Sci.* **1989**, 223, 13.
- Joseph, Y.; Ranke, W.; Weiss, W. *J. Phys. Chem. B* **2000**, 104, 3224.
- Herman, G. S.; Kim, Y. J.; Chambers, S. A.; Peden, C. H. F. *Langmuir* **1999**, 15, 3993.
- Aplincourt, P.; Bureau, C.; Anthoine, J.-L.; Chong, D. P. *J. Phys. Chem. A* **2001**, 105, 7364.
- Jenniken, H. G.; Dorlandt, P. W. F.; Kadodwala, M. F.; Kleyn, A. W. *Surf. Sci.* **1996**, 357–358, 624.
- O'Shea, J. N.; Schnadt, J.; Brühwiler, P. A.; Hillesheimer, H.; Mårtensson, N.; Patthey, L.; Krempasky, J.; Wang, C. K.; Luo, Y.; Ågren, H. *J. Phys. Chem. B* **2001**, 105, 1917.
- Amed, S. I.-U.; Perry, S. S.; El-Bjerrami, O. *J. Phys. Chem. B* **2000**, 104, 3334.